Monitoring High-Temporal-Resolution Convective Stability Indices Using the Ground-Based Atmospheric Emitted Radiance Interferometer (AERI) during the 3 May 1999 Oklahoma–Kansas Tornado Outbreak

WAYNE F. FELTZ AND JOHN R. MECIKALSKI

Cooperative Institute for Meteorological Satellite Studies, University of Wisconsin—Madison, Madison, Wisconsin

ABSTRACT

The Department of Energy Atmospheric Radiation Measurement Program has funded the development and installation of five atmospheric emitted radiance interferometer (AERI) systems around the Southern Great Plains Cloud and Radiation Test Bed located in Oklahoma and Kansas. The AERI instruments measure atmospheric emitted radiance to within 1% ambient radiance at 1 cm^{-1} spectral resolution from 520 to 3000 cm^{-1} (3–20 μm) at 10-min temporal resolution. This high-spectral-resolution radiance information is inverted through a form of the infrared radiative transfer equation to produce temperature and water vapor profiles within the planetary boundary layer (to 3 km), effectively mapping the thermodynamic state of the lower troposphere. Taking advantage of the 10-min resolution of the AERI thermodynamic profiles, the convective destabilization during the 3 May 1999 Oklahoma–Kansas tornado outbreak is analyzed. Tropospheric changes involving the rapid (on the order of 1–2 h) dissipation of a capping temperature inversion within the planetary boundary layer, increasing boundary layer moisture, and a strong upper-level short wave lead to the systematic development of severe convection on this day. The AERI systems were able to monitor the trends in bulk atmospheric stability via diagnosed quantities such as surface-based parcel equivalent potential temperature, inversion intensity, convective available potential energy, and convective inhibition. The high temporal resolution of temperature and moisture profiling and bulk stability information is unique. Special radiosonde launches (nonsynoptic) are currently the only widely used means to determine this stability information. The array of five AERI instruments within Oklahoma and Kansas (collocated with wind profilers) offers the operational forecaster a unique and important data source for the thermodynamic evolution of the boundary layer, convective instability, and numerical weather prediction model validation.

1. Introduction and motivation

The tornado outbreak in central Oklahoma and south-central Kansas on the afternoon and evening of 3 May 1999 will be remembered for several reasons: At least 62 tornadoes occurred within a 10-h period over a relatively small geographical region. One tornado (rated as F5) tracked through the southern suburbs of Oklahoma City, destroying approximately 2300 homes and businesses and causing nearly $1 billion worth of damage. By day's end, 50 persons had died, 44 in Oklahoma and 6 in the Wichita, Kansas, area.

Perhaps one of the more interesting aspects of this event was the evolution of the severe convection on this day. The precursors to such a widespread severe outbreak were not defined well from the early morning (3 May) model or surface analysis (Thompson and Edwards 2000). A consequence of this was that the risk assessment for severe weather by the Storm Prediction Center was reevaluated and upgraded several times leading up to the initiation of severe convection. The primary reason for the difficulty in forecasting the event was an underinitialized jet stream wind maximum and short wave within the operational forecast models. The features were located off of the Pacific coast of the United States at 1200 UTC 3 May 1999 (Thompson and Edwards 2000). The jet stream maximum subsequently traversed northern Mexico and did not become realized within the U.S. observation network until it was observed by several wind profilers in the southwest United States. The primary focus of this paper is not on the strong upper-level short wave, but rather is on the rapid thermodynamic destabilization that occurred within the Oklahoma–Kansas area on 3 May 1999, which assisted in initiating severe convection.

Previous studies of the preconvective environment highlight the importance of changing planetary boundary layer (PBL) heat and moisture for the initiation of deep convection (Beebe 1958; Carlson 1983; Sanders 1986; Colby 1984; Sanders and Blanchard 1993). Increasing heat and, especially, moisture lower the level

Corresponding author address: Wayne F. Feltz, CIMSS, Space Science and Engineering Center, University of Wisconsin—Madison, 1225 W. Dayton St., Rm. 239, Madison, WI 53706.
E-mail: wayne.feltz@ssec.wisc.edu

Fig. 1. The AERI located in Lamont, OK, as part of the DOE ARM program.

of free convection and increase a parcel's convective available potential energy (CAPE) (Bluestein 1993). In addition, the presence of convective inhibition (CIN, in the form of a capping inversion) may prevent the realization of this potential energy within the free troposphere (Sanders and Blanchard 1993). Up-to-date knowledge of the balance between PBL equivalent potential temperature θ_e and the intensity of the capping inversion monitored at high time resolution is clearly critical to a successful nowcast of thunderstorm occurrence.

The motivation for this paper is to demonstrate the capabilities of the atmospheric emitted radiance interferometer (AERI) instrument for identifying the changing PBL thermodynamic character at a time resolution of 10 min. Therefore, the value of the AERI instrument for operational mesoscale forecasting and postanalysis of thermodynamic destabilization during the 3 May 1999 severe thunderstorm event is explored. Using part of the array of five AERI instruments stationed across Oklahoma and Kansas as part of the Department of Energy (DOE) Atmospheric Radiation Measurement (ARM) Program, time series of vertical temperature and water vapor profiles, CAPE, and CIN are analyzed. These datasets provide a unique, real-time assessment of the preconvective atmosphere, not available from

conventional sounding observations, which are taken only at 0000 and 1200 UTC synoptic times (or in special cases an additional sounding may be launched to assess severe weather potential further).

This paper proceeds as follows: A general description of the AERI is presented in section 2, the meteorological background of the 3 May 1999 outbreak is provided in section 3, and section 4 overviews the spatially varying atmospheric conditions, as measured by AERI, over the time of severe convective development on 3 May 1999. The paper is summarized and concluded in section 5.

2. AERI overview

The AERI (Fig. 1) is a well-calibrated ground-based instrument that measures atmospheric emitted infrared (IR) radiances from the atmosphere at high spectral resolution. It is designed to perform frequent measurements, as often as 7 min apart. Because of the instrument's high spectral resolution (less than one wavenumber between 3 and 18 μm within the IR spectrum), AERI detects vertical changes in temperature and water vapor with a high degree of precision within the PBL below approximately 3 km (Feltz et al. 1998).

The retrieval of PBL temperature and moisture structure from ground-based high-spectral-resolution IR

measurements has been developed over a 10-yr period at the University of Wisconsin. Papers by Feltz (1994), Feltz et al. (1998), and Smith et al. (1990, 1993, 1999) provide much of the overview of the AERI instrument and physical retrieval algorithm development. Therefore, only a brief description of the instrument is presented as it applies to real-time data collection and the processing of convective indices.

The radiance spectra measured by the AERI contain (vertical) temperature and water vapor profile information, as documented in Feltz et al. (1998). By inverting the radiative transfer equation, these profiles can be retrieved. However, the retrieval of water vapor and temperature from radiance data is an ill-defined problem. Smith et al. (1999) have developed an iterative technique that makes use of a first-guess profile when performing a physical retrieval of the temperature and water vapor profiles. The first-guess profile is derived from a statistical methodology that is based on a regression of 1159 clear radiosondes launched at the Southern Great Plains (SGP) Cloud and Radiation Test Bed (CART) central facility (near Lamont, Oklahoma), between 25 July 1994 and 10 May 1996, and a forward calculation at AERI spectral resolution using each of these radiosondes. The forward model is a necessary component for performing AERI retrievals in real time (within a 10-min window) and is obtained by regressing optical depth from a line-by-line transmittance model [in this case "FASCODE" described in Clough et al. (1981)] against parameters obtained by temperature and water vapor mixing ratio profiles. This first-guess regression of temperature and moisture is very robust because it has sampled a wide range of meteorological events that passed through the SGP CART site domain. This first guess of temperature and moisture is therefore based upon site-specific climatic data; it is then subsequently passed through the physical retrieval algorithm described within Smith et al. (1999). Because of the strength of the IR signal at the surface from emission within the lower atmosphere, the weighting functions (functions that describe the emission of a particular band of IR radiation with height) become very broad at 2.5–3 km. Therefore, the retrievals using only AERI data are limited to these altitudes, becoming more spurious above 3 km as the amount of information measured by AERI decreases.

Complete tropospheric profiling can be accomplished by using physically retrieved temperature and water vapor profiles from the Geostationary Operational Environmental Satellite's (GOES) sounder brightness temperature data (Menzel et al. 1998; Ma et al. 1999). The GOES profiles serve as the first guess of the atmospheric state from the upper PBL (2.5 km) to the tropopause. The AERI statistical first guess is blended into the GOES sounder physical retrieval between 2 and 3 km in the vertical. This improves the first guess used for the AERI physical retrieval algorithm in the upper PBL over using statistics derived from forward model cal-

culations alone. The GOES sounder retrievals, in contrast to the upward-looking AERI, are more sensitive to the upper- and midtropospheric temperature and humidity as its weighting functions broaden out significantly toward the surface. The combination of AERI and GOES retrievals provides an excellent synergistic blend of the two passive retrievals for two reasons: First, the physical retrieval algorithm used by the AERI is able to modify the profiles retrieved by the GOES in a region where the AERI's retrieval algorithm performs well, within the PBL. Second, the AERI retrieves profiles in the more rapidly changing thermodynamic structure of the PBL at temporal resolutions appropriate for this part of the troposphere; the GOES retrievals are hourly in the middle and upper troposphere where meteorological conditions change more slowly.

In order for the GOES to retrieve temperature and water vapor profiles, the sky conditions must be clear or broken (at least four pixels in a 3×3 array around the central point of interest must be determined to be clear; each pixel is 10 km in resolution at the GOES subsatellite point). It should be noted that GOES retrievals use National Centers for Environmental Prediction Eta Model 6–18-h forecast temperature and moisture profiles for the first guess. GOES adjusts the Eta temperature profile very little over land where the radiosonde network is relatively more dense (Ma et al. 1999). Therefore the temperature information above the PBL within the hybrid (AERI + GOES) first guess is primarily coming from the Eta forecast fields. During some synoptic situations, overcast skies will prevent the retrieval of water vapor and temperature profiles from GOES data. In these cases, a statistical first guess is used to allow the AERI to profile under the cloud deck. However, if the clouds are too low (<1.0 km), the IR signal from the clouds overwhelms the weaker water vapor and temperature signatures, and thus the algorithm is unable to converge (Smith et al. 1999).

Comparisons to collocated radiosondes at the SGP CART site with AERI + GOES retrievals indicate root-mean-square differences of 1 K for temperature and 6%–8% absolute water vapor within the PBL, as reported in Feltz et al. (1998, 2002, manuscript submitted to *J. Appl. Meteor.*, hereinafter FHKWR), and Turner et al. (2000).

The disadvantage of a passive remote sensing instrument that senses within the IR spectrum is that precipitation and low clouds saturate the signal, providing very little useful thermodynamic profiling information. (However, cloud emissivity and temperature can certainly be measured.) The problem is not serious for nowcasting severe weather, considering that, to destabilize the lower atmosphere, direct heating from solar radiation is often needed. This inherently means that there will be breaks within the cloudiness for profiling opportunities. The 10-min resolution takes advantage of these opportunities. The AERI retrieval algorithm is also able to calculate profiles to cloud base, which allows
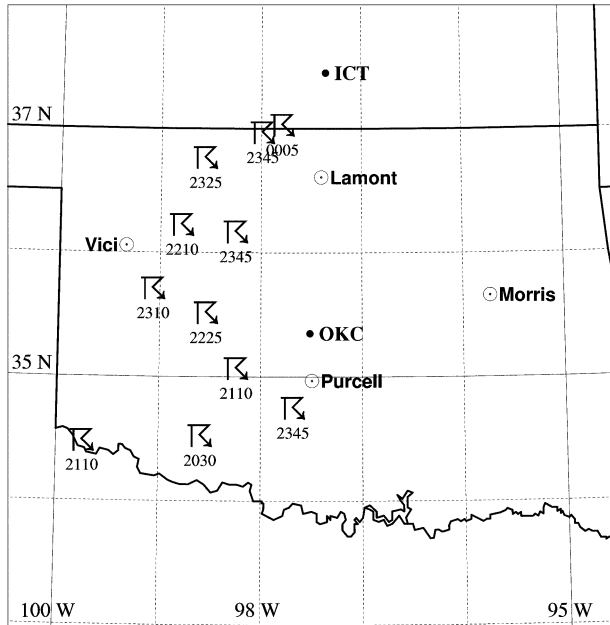
FIG. 2. Map of convective initiation times (UTC) over the OK and KS area on 3 May 1999, subjectively analyzed from 1-km *GOES-8* visible imager data. Thunderstorms symbols indicate locations of initial thunderstorm development. "OKC" is Oklahoma City.

for the monitoring of average θ_e with the lowest 100 hPa of the atmosphere, which is important for calculating most bulk stability indices.

3. Meteorological background

Shown in Fig. 2 are the locations and times of the initial convective developments across the region. Convective initiation time and location were subjectively determined from 1-km *GOES-8* visible satellite imagery. Also shown in Fig. 2 are the locations of four (Lamont, Morris, Purcell, Vici) of the five AERI instruments deployed within Oklahoma. The three AERI systems relevant to this study are those collocated with the National Weather Service 449-MHz wind profilers at Lamont, Vici, and Purcell, Oklahoma.

Figure 3 presents a plot of surface dewpoint temperature (°F) and wind direction/velocity (kt) at 2000 (Fig. 3a), 2100 (Fig. 3b), and 2300 UTC (Fig. 3c) over 1-km-resolution visible satellite images at 2015, 2115, and 2315 UTC 3 May 1999, respectively. Figure 3d shows the 0015 UTC 4 May 1999 visible imagery along with four AERI instrument locations (which are labeled as small squares in Figs. 3a–d).

Upon inspection of the dewpoint and wind data (Figs. 3a–c), nearly all the deep convection formed east of a north–south line centered on Vici, Oklahoma, on the far western edge of the region of relatively high surface moisture (dewpoint temperatures about 63°–70°F; 17.2°–21.1°C). Although a surface dryline was present, it did not seem to be the focus for initial convective

development. The first cumulonimbus to form were those near 34.5°N, 98.6°W (near Lawton, Oklahoma, noted in Fig. 3d) at 2030 UTC. These storms were at least 100 km east of the eastern edge of the drier air [note regions along the Texas Panhandle–Oklahoma border in which dewpoints were below 60°F (15.6°C); Fig. 3b]. However, the initial convective development at 2030 UTC occurred near the point of highest θ_e in western Oklahoma (Fig. 4a).

Once convection first developed, the event was characterized by the rapid formation of supercell thunderstorms, over a 2–6-h period. The discussion will be focused on the development of convection that affected areas near Purcell and Oklahoma City, between 2000 and about 2130 UTC, and over north-central Oklahoma and south-central Kansas, between roughly Lamont, Oklahoma, and Wichita, Kansas. Convection in this second area developed rapidly between 2300 UTC 3 May and 0015 UTC 4 May, such that locations experiencing partly cloudy sky conditions at 2315 UTC (Fig. 3c) were reporting severe weather conditions by 0015 UTC (Fig. 3d; i.e., in regions west of Lamont).

Figure 4b also shows a broad area of θ_e convergence (as surface winds veered from southerly to more southsouthwesterly) into western Oklahoma. Dewpoint temperatures across most of the region to be affected by deep convection were generally from 63° to 70°F (18°–20°C). However, CAPE values were very large, between 2500 and 4000 J kg^{-1} (see Fig. 6). Convection that formed between 2030 UTC 3 May and 0015 UTC 4 May was even farther east of any discernible surface boundary or moisture discontinuity. Therefore, from analysis of surface dewpoint, wind, and θ_e convergence information, no well-defined surface feature appears to have played a significant role in determining the initiation points (in space and time) for the severe convection of 3–4 May 1999.

Turning then to the middle troposphere, Figs. 5a and 5b show evidence of a short wave and associated jet streak at 500 hPa. The short wave, denoted by a dashed line in Figs. 5a and 5b, is seen to amplify over the 12-h period of this figure. The short wave becomes well defined from Idaho to New Mexico by 0000 UTC 4 May, and the flow became more diffluent over the region of interest (Fig. 2). It may be argued from Fig. 5b that Oklahoma lies directly beneath the left-front quadrant ("exit region") of the jet extending from Arizona to southwest Texas (Thompson and Edwards 2000). Yet, similar to the surface data, there is relatively little evidence in these data that would help a forecaster to isolate precisely when and where thunderstorms may form. Because the location of thunderstorm initiation was difficult to identify in surface and upper-air data, it becomes important to have high-temporal-stability information of the PBL, exactly that provided by the AERI instruments.

From the surface and upper-air data, the following can be concluded: 1) sufficient energy (CAPE) was
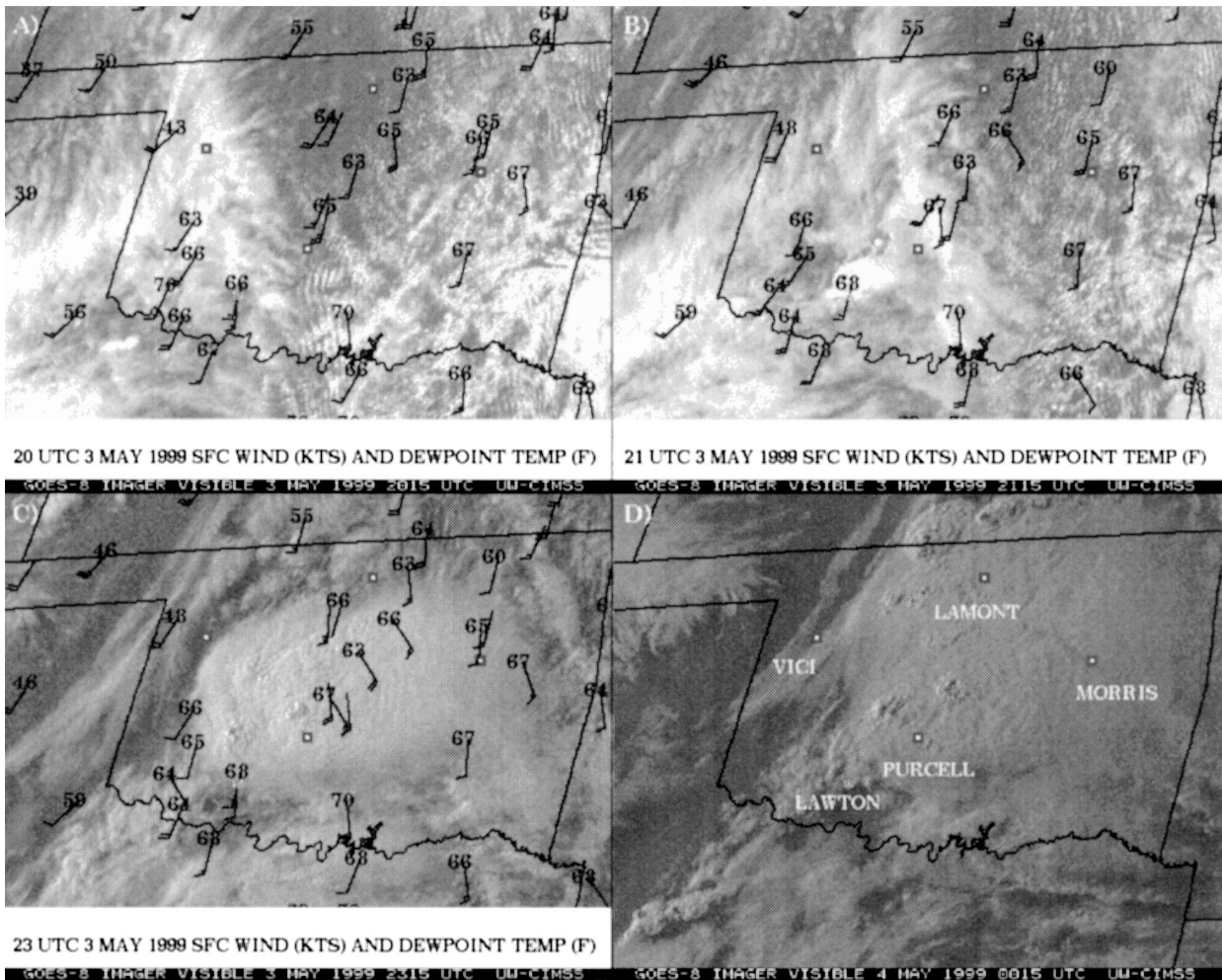
FIG. 3. *GOES-8* visible satellite image for 2000–2400 UTC 3 May 1999 with locations of the AERI systems plotted (squares). Surface-based dewpoint (°F) and wind (kt) measurements are also indicated. Detailed time information for (a)–(d) is given in the text.

available for deep cumulus development, 2) very little evidence exists within the surface data to suggest when and where deep convection would initiate, and 3) significant diffluence in the presence of strengthening upper-level winds to the southwest and west of the target area was present to help to sustain and to maintain severe convection, yet the strength of this diffluence was not necessarily foreseen at 1200 UTC 3 May 1999. Hence, the forecaster of this event was significantly challenged to determine where deep convection would develop.

4. AERI and the preconvective environment

Figures 6a–c present the time series of θ_e, CIN, and CAPE from 1200 UTC 3 May to 0000 UTC 4 May 1999 for three AERI sites, Vici (blue), Lamont (red), and Purcell (black). The locations of these stations relative to the initiation of convection are presented in Fig. 2. The CIN and CAPE stability indices have been derived from the average θ_e (Fig. 6a) within the lowest 100 hPa of the atmosphere.

Several items are of immediate interest in Fig. 6. First, since the AERI instrument can make useful profiles only under partly cloudy or clear-sky conditions, missing data appear as straight lines between retrieval points (+ symbols). Even though all 10-min profiles are not available because of low clouds, time tendencies of the indices are followed by the intermintant profiles retrieved between low clouds. This is actually a challenging retrieval situation. Many other convective destabilization events that the AERI systems have monitored were associated with clear-sky conditions leading up to thunderstorm development.

Also in Fig. 6, the red and black circles represent θ_e, CIN, and CAPE values calculated directly from radiosonde soundings. The red circles correspond to data collected at the AERI site in Lamont, and the black circles are data collected from launches at Norman, Oklahoma (south of OKC by about 20 km), which correspond to the AERI + GOES data at Purcell.

From Fig. 6a, the parcel θ_e generally increased with time, especially at Lamont and Purcell, with a notable

(a)

3 MAY 1999 2000 UTC SFC EQUIVALENT POTENTIAL TEMPERATURE

(b)

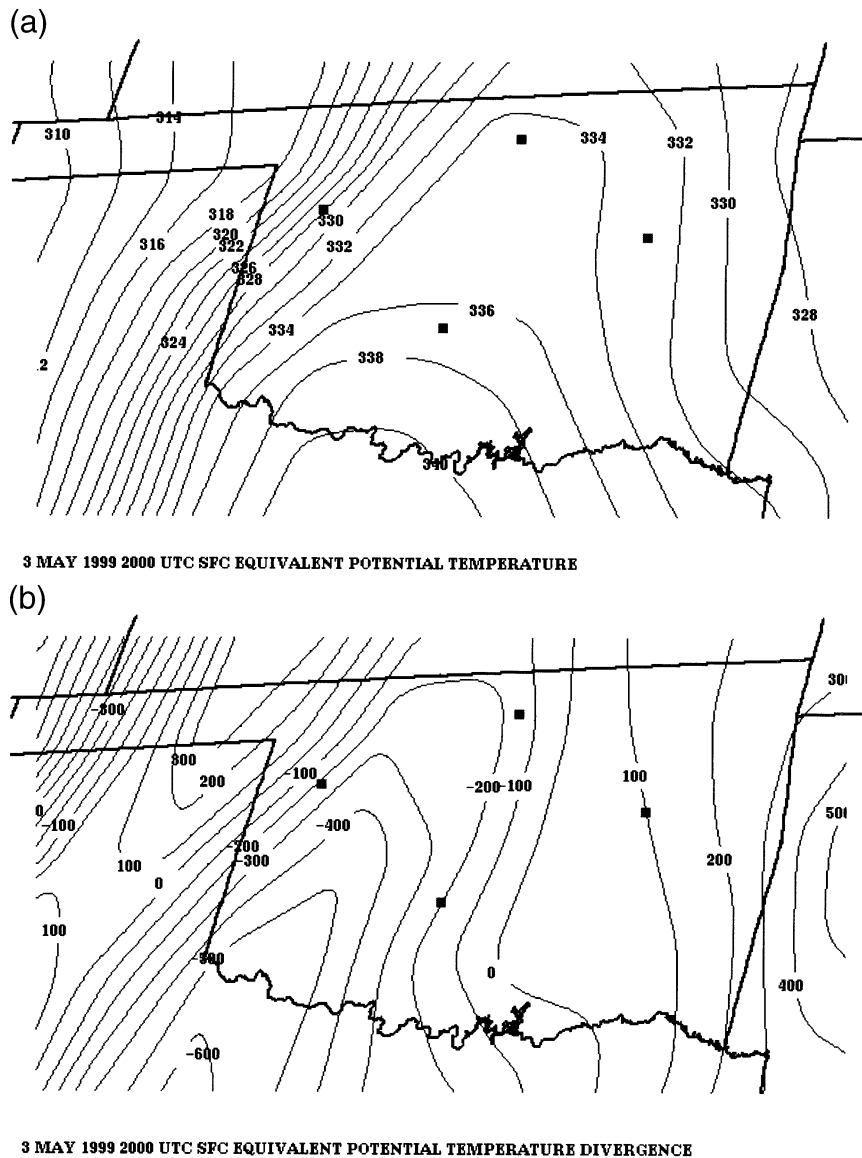3 MAY 1999 2000 UTC SFC EQUIVALENT POTENTIAL TEMPERATURE DIVERGENCE

FIG. 4. (a) Equivalent potential temperature (K) and (b) equivalent potential temperature divergence (K s^{-1}) at 2000 UTC on 3 May 1999. Negative divergence is convergence.

decrease in θ_e seen at Vici (in west-central Oklahoma) occurring abruptly after 2200 UTC. This decrease at Vici is correlated with an intrusion of drier surface-layer air from the west. It is clear that the agreement between collocated radiosonde and AERI + GOES temperature and moisture (to construct a θ_e) is very high. Note that the θ_e calculated in Fig. 4a is just the surface-based measurement; the AERI and radiosonde values are derived from the first 100 hPa of the atmosphere (bulk θ_e). It is also seen that the higher occurrences of clear-sky conditions at Vici lead to more frequent AERI + GOES retrievals.

Figures 6b and 6c highlight the changing CIN and CAPE within the preconvective environment. CIN values were negative at all three sites, indicating the general presence of a capping inversion across Oklahoma on this day. Convective inhibitions at Purcell were lower (smaller negative) over the 12-h period, suggesting that this region of Oklahoma was most prone to thunderstorm occurrence. The rapid lowering of CIN at Purcell between about 1900 and 2100 UTC corresponds to the rapid development of thunderstorms in regions south and west of OKC during this time period (Fig. 3b). Also important are the trends in CIN at both Vici and Lamont; at Vici, CIN decreased from -300 to near -50 J kg^{-1} between 1800 and 2200 UTC before increasing rapidly to -120 J kg^{-1} again by 2300 UTC 3 May. The decrease in CIN is likely due to the coincident increase in θ_e; the dry-air advection into this region after 2200 UTC leads to the increase in CIN. The lack of deep convection

(a)
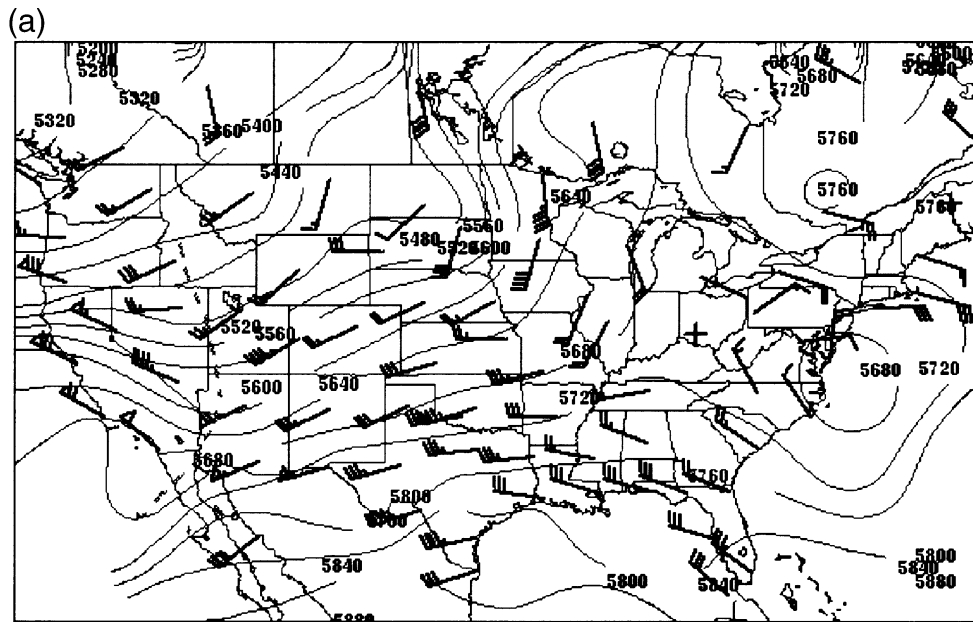
3 MAY 1999 1200 UTC 500 MB HEIGHTS/WINDS

(b)
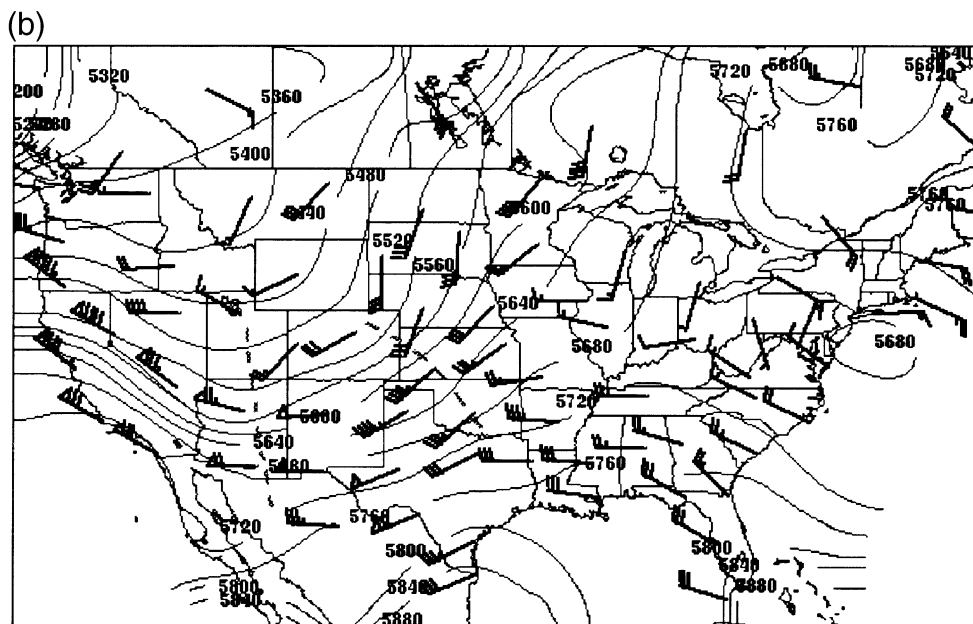
4 MAY 1999 0000 UTC 500 MB HEIGHTS/WINDS

FIG. 5. Geopotential heights (m, solid lines) and wind velocities (m s^{-1}) from radiosonde data at 500 hPa for (a) 1200 UTC 3 May 1999 and (b) 0000 UTC 4 May 1999. Dashed line in (b) denotes trough axis.

at Vici is corroborated by CIN remaining large. Note that, although high temporal monitoring of CIN is useful for operational forecaster nowcasting, CIN is only one part of the thunderstorm initiation problem. Parcel lift may be high enough to overcome CIN (Thompson and Edwards 2000).

At Lamont, CIN decreased gradually from −180 and −50 J kg^{-1} from 1900 to about 2300 UTC 3 May before

rapidly decreasing to −25 J kg^{-1} by 2330 UTC. It was at 2330 UTC that no additional AERI + GOES profiles were possible because of the dense anvil cirrus shield over the station (Figs. 3c and 3d). The collocated Lamont radiosonde at 2330 UTC shows that CIN remained low, near −50 J kg^{-1}, at 2345 UTC 3 May. Based on GOES satellite imagery in Fig. 3c, thunderstorm development occurred very rapidly in north-central
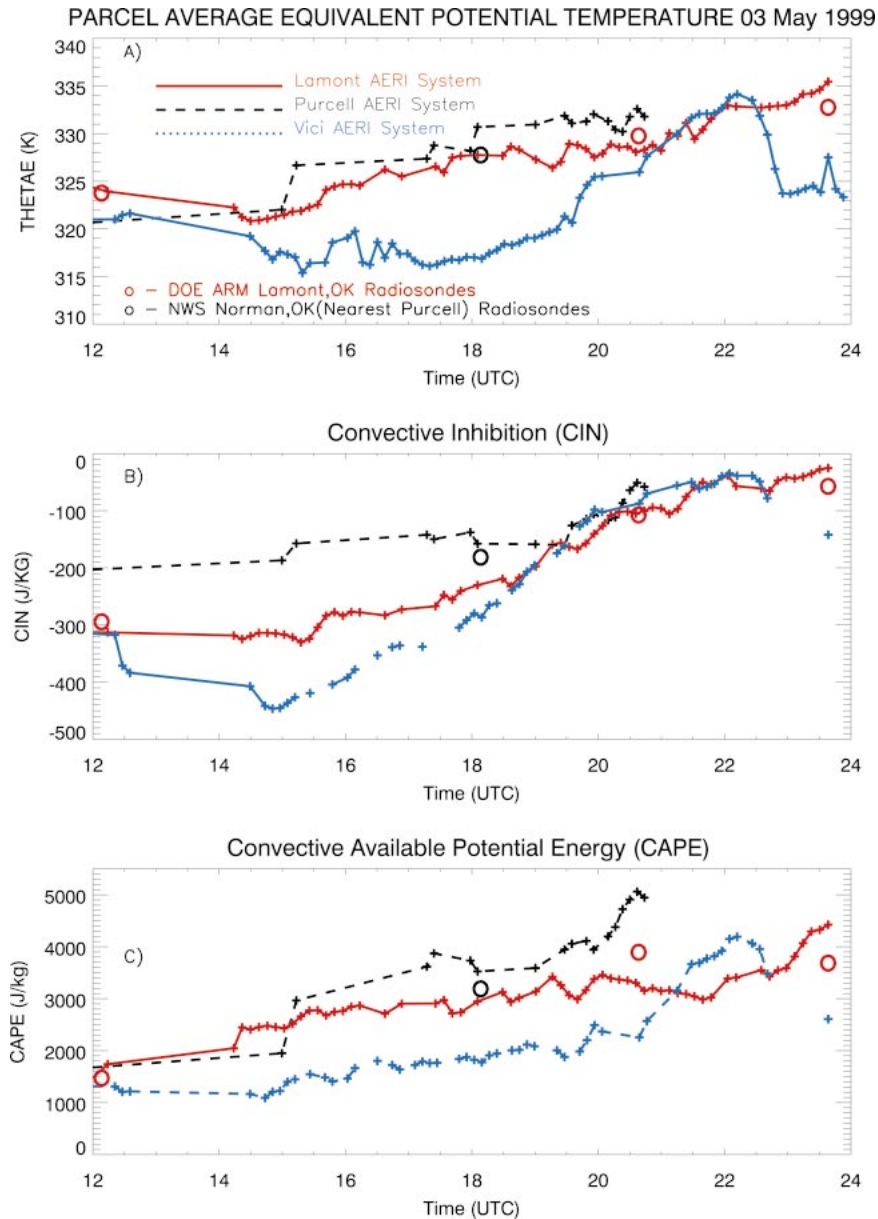
PARCEL AVERAGE EQUIVALENT POTENTIAL TEMPERATURE 03 May 1999

FIG. 6. Time series of (a) equivalent potential temperature (K), (b) CIN (J kg^{-1}), and (c) CAPE (J kg^{-1}) derived from AERI + GOES retrievals (+) for Purcell, Lamont, and Vici. Validation radiosonde data points are indicated by circles.

Oklahoma and south-central Kansas between 2315 UTC 3 May and 0000 UTC 4 May. The trend in CIN at Lamont is striking and was an important precursive indicator of the thunderstorm development, considering the development that had occurred over central and western Oklahoma already. This CIN tendency is very similar to the Purcell AERI CIN time tendency of only 3 h earlier. The strength of the AERI instrument is therefore demonstrated very well here for assessing, in real time, the changing preconvective environment in this thunderstorm case.

CAPE tendencies in Fig. 6c show a general trend toward increasing energies, beginning near 1400 UTC, at all these stations. Again, these data show that just prior to the occurrence of deep convection (by about 1 h) at Lamont, CAPE increased more rapidly (to near 4500 J kg^{-1}). The CAPE near Purcell gradually increased from near 2000 at 1500 UTC to 4000 at 2000 UTC. A rapid increase in CAPE to near 5000 J kg^{-1} was observed by the AERI retrievals between 2000 and 2100 UTC just near the time of convective initiation to the southwest of Purcell. The rapid increase in CAPE to around 4000 J kg^{-1} at Vici centered on 2200 UTC was followed by an abrupt decrease to near 2200 J kg^{-1}
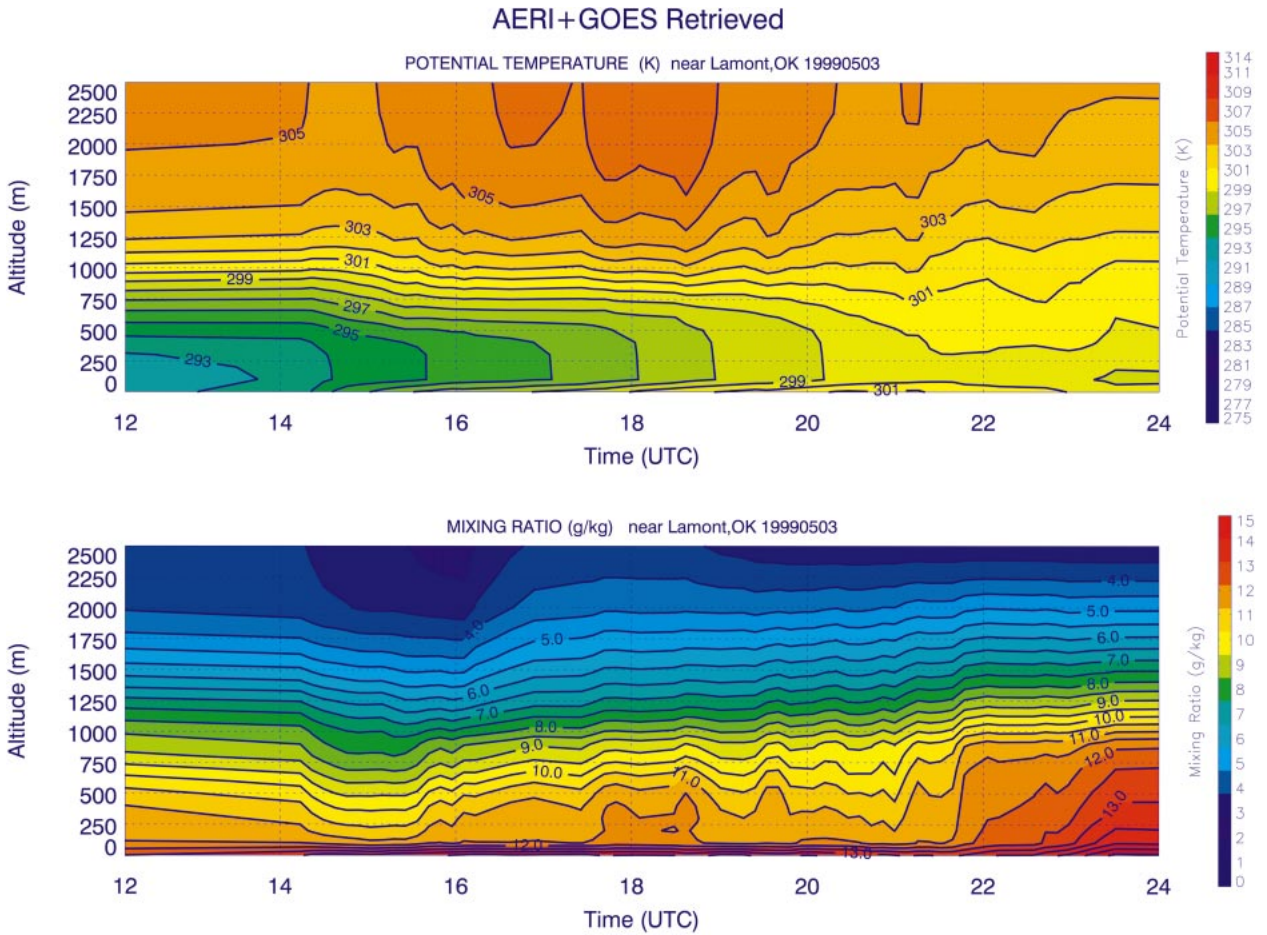
FIG. 7. Time–height cross section of 10-min-resolution AERI-derived potential temperature (K) and water vapor mixing ratio (g kg^{-1}) from 1200 to 2400 UTC 3 May 1999 near Lamont.

by 0000 UTC 4 May, coincident with decreasing parcel θ_e and hence an increase in (negative) CIN. Collocated radiosonde-estimated CAPE values were somewhat more poorly correlated with the AERI + GOES data, which is likely due to the reliance on a model-derived temperature profile above 3 km (GOES has little influence on the first-guess temperature profile, which in this case was from the Eta Model).

As shown in Fig. 6, the near-steady-state θ_e measurements between 1900 and 0000 UTC at Lamont and the rapid decrease in convective inhibition are indicative of the capping inversion eroding with time. A time–height cross section of AERI + GOES retrieved potential temperature and water vapor mixing ratio (Fig. 7) from Lamont indicates some increase in the amount and depth of moisture, as well as the rapid decrease in static stability between 2000 and 0000 UTC. The decrease in the vertical gradient of potential temperature is readily apparent between 1900 and 2200 UTC at approximately 1 km in altitude. As a way of highlighting the inversion erosion captured by the AERI + GOES retrievals, Figs. 8a–c present the observed Lamont measured soundings

(Fig. 8a), along with the AERI + GOES soundings at two preconvective times for Lamont (Fig. 8b) and Purcell (Fig. 8c). Data to 300 hPa are shown; data above 700 hPa on the AERI + GOES plots are almost exclusively derived from Eta Model temperature profiles. The destruction of the capping inversion is seen below about 830–800 hPa.

Figure 8 shows the following:

1) At Lamont, between 2027 and 2327 UTC (the two available soundings; Fig. 8a), a dramatic reduction in the inversion strength occurred in the 830-800-hPa layer.
2) AERI + GOES derived soundings at Lamont (Fig. 8b) show the reduction in the inversion (between ~850 and 800 hPa) over the period 1954–2351 UTC (the closest AERI retrievals to the two radiosonde launches). The smoothing of the inversion over a deeper layer as compared with the radiosondes is due to the decrease of the AERI + GOES vertical resolution and effectiveness with altitude. The decrease in inversion strength is very much evident,
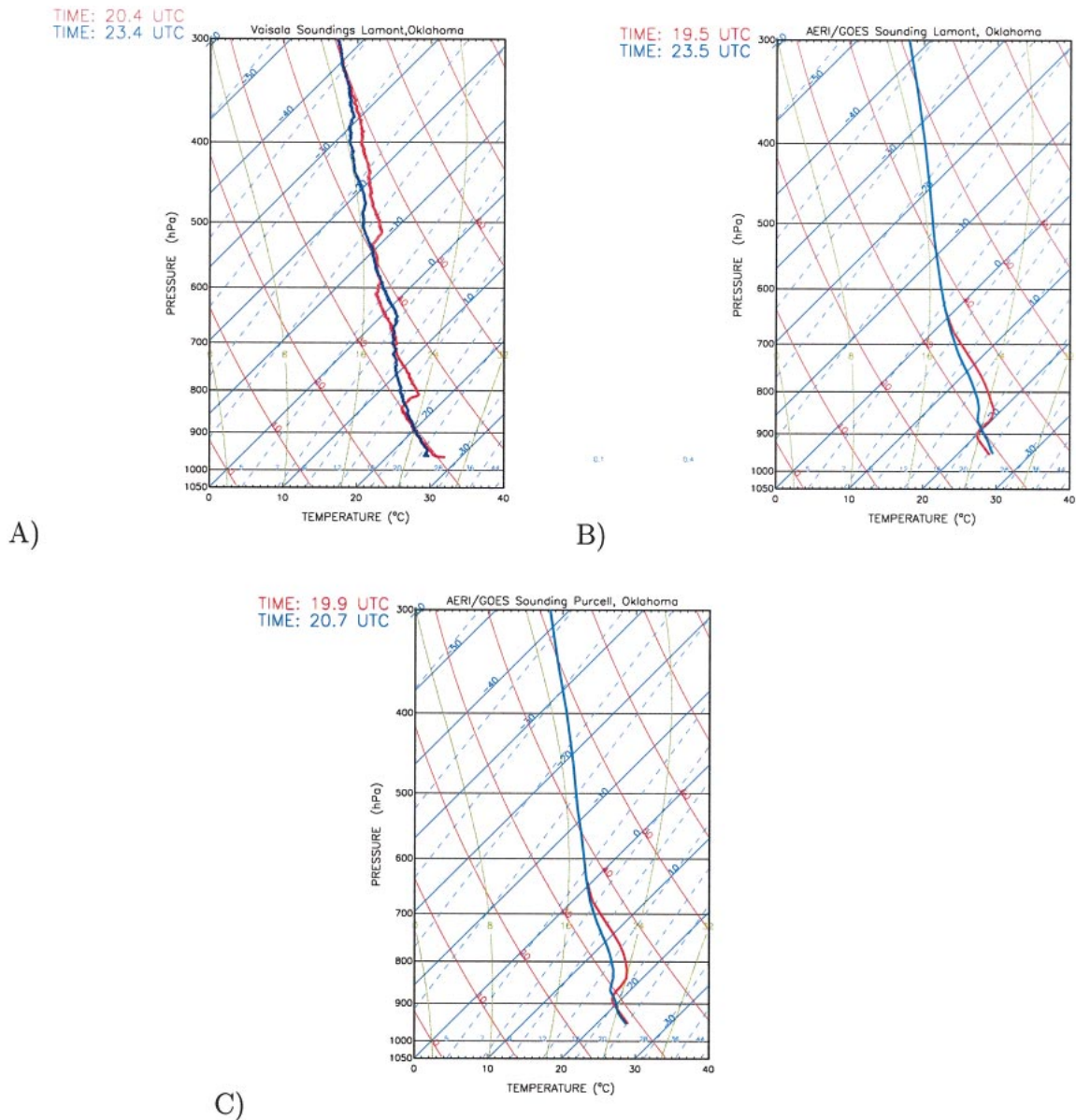
FIG. 8. A comparison of (a) temperature profiles from two radiosondes launched in Lamont and AERI + GOES temperature retrieval profiles near (b) Lamont and (c) Purcell. All indicate erosion of the PBL temperature inversion.

and, at time resolutions of 10 min, animations of consecutive sounding images show the trend toward a decreasing inversion strength.

3) Similar to Lamont, the Purcell AERI + GOES profiles (Fig. 8c) demonstrate very effectively the sharp decrease in the inversion strength (between 875 and about 680 hPa) that occurred in less than 1 h, from 1956 to 2044 UTC.

The AERI profiles were capable of providing a forecaster a near-real-time perspective of the changing PBL that could only be duplicated by having very frequent radiosonde launches. Animations of these data (available at the time of writing at http://cimss.ssec.wisc.edu/ aeriwww/aeri/) highlight the continuum of changes to both atmospheric stability and the inhibiting factors for the occurrence of thunderstorms.

5. Summary and conclusions

This paper has shown high-temporal-stability indices and profiling data from the AERI instrument network in the Oklahoma area during the 3 May 1999 tornado outbreak. This upward-pointing interferometer offers a high-temporal-resolution view of the atmospheric PBL up to about 3 km. From an operational perspective, AERI retrievals can monitor PBL atmospheric stability

and temperature inversion magnitude. Convective indices formed from AERI retrievals are designed to identify both the energy available and the energy inhibiting the development of deep (and in this case severe) convection for the 3 May 1999 Oklahoma and Kansas tornado outbreak; these data provide an excellent example of how AERI can be used to chart the evolution of the preconvective environment.

The analysis shows that the AERI-observed CIN tendency information across the Oklahoma and Kansas region diminished in concert with severe storm development. The erosion of the capping inversion was seen to occur firstly in southwestern Oklahoma, later in central Oklahoma, and finally in south-central Kansas. Considering the difficulty in linking surface and tropospheric synoptic-scale forcing (in the form of a dryline, and 500-hPa jet streak) directly to the occurrence of severe storm development, the real-time information offered by AERI provides some insight about the stability index tendency and capping inversion strength just prior and during the outbreak. In this case, the real-time AERI stability information would not have enhanced forecasters' knowledge of exact thunderstorm development because the systems were not located near the Lawton, Oklahoma, area. However, stability tendency and AERI location stability comparisons may help the forecaster to define better the region of expected convective development. This single severe weather episode is notorious for the strength of the tornadoes and the destruction they caused, but many other less dramatic examples of rapid lower-tropospheric destabilization have been recorded by the AERI system during the spring and summer of 1999 and 2000. A more thorough quantitative comparison of AERI-derived stability indices to radiosondes for the 1999/2000 severe weather season will be a subject of a future paper (FHKWR). The AERI instrument has now been commercialized and plans have been made to supplement the DOE ARM AERI network along the Gulf of Mexico coast to monitor return flow water vapor into the center of the United States. Near-real-time AERI retrievals have been made available via the Internet (http://cimss.ssec.wisc.edu/aeriwww/aeri).

REFERENCES

Beebe, R. G., 1958: Tornado proximity soundings. *Bull. Amer. Meteor. Soc.,* **39,** 195–201.

Bluestein, H. B., 1993: *Observations and Theory of Weather Systems.* Vol. 2. *Synoptic-Dynamic Meteorology in Midlatitudes,* Oxford University Press, 594 pp.

Carlson, T. N., S. G. Benjamin, G. S. Forbes, and Y. F. Li, 1983: Elevated mixed layers in the regional severe storm environment: Conceptual models and case studies. *Mon. Wea. Rev.,* **111,** 1453–1473.

Clough, S. A., F. X. Kneizys, L. S. Rothman, and W. O. Gallery, 1981: Atmospheric spectra transmittance and radiance: FASCODE1B. *SPIE Atmos. Transmission,* **277,** 152.

Colby, F. P., Jr., 1984: Convective inhibition as a predictor of convection during AVE-SESAME II. *Mon. Wea. Rev.,* **112,** 2239–2119.

Feltz, W. F., 1994: Meteorological applications of the atmospheric emitted radiance interferometer (AERI). M.S. thesis, Dept. of Atmospheric and Oceanic Sciences, University of Wisconsin—Madison, 87 pp. [Available from Schwerdtfeger Library, University of Wisconsin—Madison, 1225 W. Dayton St., Madison, WI 53705.]

——, W. L. Smith, R. O. Knuteson, H. E. Revercomb, H. M. Woolf, and H. B. Howell, 1998: Meteorological applications of temperature and water vapor retrievals from the ground-based Atmospheric Emitted Radiance Interferometer (AERI). *J. Appl. Meteor.,* **37,** 857–875.

Ma, X. L., T. J. Schmit, and W. L. Smith, 1999: A nonlinear physical retrieval algorithm—Its application to the *GOES-8/9* sounder. *J. Appl. Meteor.,* **38,** 501–513.

Menzel, W. P., F. C. Holt, T. J. Schmit, R. M. Aune, A. J. Schreiner, and D. G. Gray, 1998: Application of *GOES-8/9* soundings to weather forecasting and nowcasting. *Bull. Amer. Meteor. Soc.,* **79,** 2059–2077.

Sanders, F., 1986: Temperatures of air parcels lifted from the surface: Background, application, and monograms. *Wea. Forecasting,* **1,** 190–205.

——, and D. O. Blanchard, 1993: The origin of a severe thunderstorm in Kansas on 10 May 1985. *Mon. Wea. Rev.,* **121,** 133–148.

Smith, W. L., and Coauthors, 1990: GAPEX: A Ground-based Atmospheric Profiling Experiment. *Bull. Amer. Meteor. Soc.,* **71,** 310–318.

——, R. O. Knuteson, H. E. Revercomb, F. Best, R. Dedecker, and H. B. Howell, 1993: GB-HIS: A measurement system for continuous profiling of boundary layer thermodynamic structure. Preprints, *Eighth Symp. of Meteorological Observations and Instrumentation,* Anaheim, CA, Amer. Meteor. Soc., J180–J183.

——, W. F. Feltz, R. O. Knuteson, H. E. Revercomb, H. M. Woolf, and H. B. Howell, 1999: The retrieval of planetary boundary layer structure using ground-based infrared spectral radiance measurements. *J. Atmos. Oceanic Technol.,* **16,** 323–333.

Thompson, R. L., and R. Edwards, 2000: Overview of environmental conditions and forecast implications of the 3 May 1999 tornado outbreak. *Wea. Forecasting,* **15,** 682–699.

Turner, D. D., W. F. Feltz, and R. A. Ferrare, 2000: Continuous water vapor profiles from operational ground-based active and passive remote sensors. *Bull. Amer. Meteor. Soc.,* **81,** 1301–1317.